Available online at www.sciencedirect.com
ScienceDirect
Nuclear Physics A 00 (2020) 1–4
Nuclear Physics A
www.elsevier.com/locate/procedia

XXVIIIth International Conference on Ultrarelativistic Nucleus-Nucleus Collisions
(Quark Matter 2019)

Recent Measurements of Heavy Quarkonium Production in Au+Au, p+Au and p+p Collisions at STAR

Yanfang Liu, for the STAR Collaboration

Physics and Astronomy Department and Cyclotron Institute, Texas A&M University

Abstract

Heavy quarkonia are useful probes of the quark-gluon plasma, where quarkonium dissociation is expected at high enough temperature. Indeed, such a suppression is clearly present in the latest STAR measurements of J/ψ production in Au+Au collisions. The suppression is observed to have little dependence on p_T, although cold-nuclear matter (CNM) effects, such as shadowing, anti-shadowing and nuclear absorption can play a significant role at low p_T. Measurements of the J/ψ production in p+A collisions can help us to disentangle the CNM effects from the hot medium effects in A+A collisions. In these proceedings, we will present the measurement of J/ψ production in p+Au collisions at $\sqrt{s_{NN}}$ = 200 GeV by the STAR experiment. In addition, we will present recent STAR measurements of J/ψ and Υ production in p+p collisions including their dependence on the charged-particle multiplicity at mid-rapidity. These measurements are important for understanding the mechanism of the heavy quarkonium production in elementary nucleon-nucleon collisions and the interplay of soft and hard processes.

Keywords: STAR, J/ψ, Υ

1. Introduction

At extremely high temperature and/or density, normal nuclear matter will transition into a new state of matter, which is called the quark-gluon plasma (QGP). In nature, it is believed the universe existed in the QGP phase for the first few microseconds after its birth. Nowadays, particle accelerators at RHIC and the LHC can create a QGP, which is the hottest man-made matter, in experiments. One important method to study the properties of this matter is to use heavy quarkonia. The original idea was that the formation of the QGP would lead to a screening of the linear confining term of the heavy quark-antiquark potential, which in turn leads to the dissociation of the J/ψ. Therefore, suppression of the J/ψ yields in heavy-ion collisions can be used as a signature of the QGP formation [1]. However, the physics turned out to be much richer than this simple picture. Besides color screening, there are other hot-medium effects such as quasi-free [2] and gluon dissociation processes [3] playing important roles in the dissociation mechanism of the quarkonia. Also, in addition to the dissociation, the recombination of a heavy quark-antiquark pair leads to the regeneration of a quarkonia in the medium. Moreover, there are also cold-nuclear matter (CNM) effects, such as from the nuclear parton distribution functions (nPDFs) [4] and nuclear absorption [5, 6]. In addition, hadronic comover dissociation [7] can also play a role in CNM. In order to understand and disentangle all these contributing effects, systematic studies are not only required in Au+Au collisions, but also in p+Au

and p+p collisions. Therefore, in these proceedings, we will try to illustrate the progress of measurements in these three systems in the STAR experiment and illustrate how it helps us to understand the quarkonium dynamics in the QGP. There are several data samples analyzed: Au+Au collisions at $\sqrt{s}$ = 200 GeV; p+Au collisions at $\sqrt{s}$ = 200 GeV; and p+p collisions at $\sqrt{s}$ = 200/500 GeV.

2. Method

Heavy quarkonia are usually measured through dilepton decay channels and at the STAR experiment, we use dielectron and dimuon to reconstruct the invariant mass spectra of the J/ψ and Υ. The relevant subdetectors in STAR to reconstruct the electron and muon candidates are: the time projection chamber which measures track for particle's momentum and energy loss for particle identification and covers $|\eta| < 1.0$; the time of flight detector which measures particles' flight time for particle identification covering $|\eta| < 1.0$; the barrel electron-magnetic calorimeter which triggers on and identifies high-p_T electrons in $|\eta| < 1.0$; the muon telescope detector which triggers on and identifies muons and covers $|\eta| < 0.5$ and 45% in $0 \leq \Phi < 2\pi$; and the vertex position detectors which provide the main minimum-bias trigger, the event start time, and cover $4.24 \leq |\eta| \leq 5.1$.

3. Results

3.1. J/ψ production in Au+Au collisions

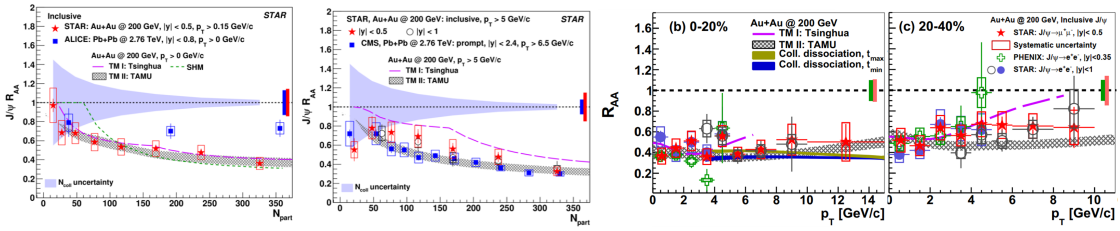

Fig. 1. Left panels:J/ψ R_{AA} as a function of the number of participants for low p_T and high p_T. The red stars are from 200 GeV Au+Au collisions at RHIC and the blue squares are from 2.76 TeV Pb+Pb collisions at the LHC [8]. Right panels: J/ψ R_{AA} as a function of p_T in selected centrality bins [8].

The "nuclear modification factor" (R_{AA}) is used to quantify the medium effects of the quarkonium production in Au+Au collisions which is defined as

$$R_{AA} = \frac{dN_{AA}}{\langle N_{\rm coll}\rangle dN_{pp}}. \quad (1)$$

It is the yield of J/ψ measured in Au+Au collisions (dN_{AA}) for a p_T range and a rapidity range, divided by the yield measured in p+p collisions (dN_{pp}), scaled by the mean number of binary collisions ($N_{\rm coll}$) in the Au+Au collisions.

The results from the STAR experiment are shown in Fig. 1. The first panel is the R_{AA} as a function of number of participants with lower p_T cut, $p_T > 0.15$ GeV/c, thus dominated by the low-p_T contribution. It shows more suppression at RHIC than at the LHC in the central collisions. This is due to the smaller production cross section for charm quarks at RHIC and therefore the regeneration at RHIC is smaller [9]. The second panel is the R_{AA} with higher p_T cut, $p_T > 5$ GeV/c, which shows both RHIC and the LHC having strong suppression in the central and semi-central collisions. As shown in the right two panels (details see Ref [8]), there is no strong p_T dependence of R_{AA} in central and semi-central collisions. There is an interplay of different effects: the formation time effect leads to less dissociation at high p_T, while at low p_T the regeneration plays a significant role. For details about the model calculations, please refer to [8].

The physics discussed above is dominated by the hot-medium effects. However, besides the hot-medium effects, there are also CNM effects, such as shadowing and nuclear absorption, which will also affect the final results of the R_{AA}. In order to disentangle the hot-medium effects and the CNM effects, we study the p+Au collisions where the final results are dominated by CNM effects.

3.2. J/ψ production in p+Au collisions

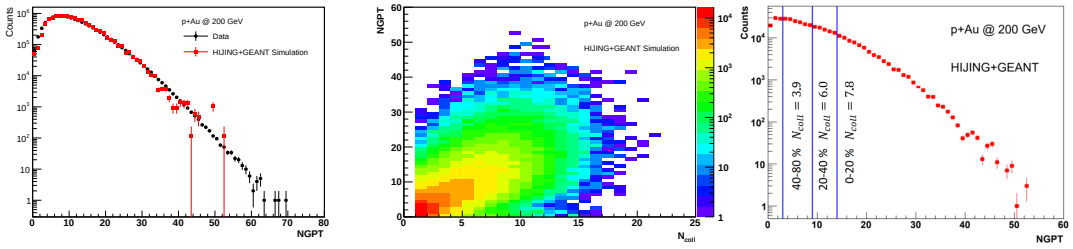

Fig. 2. Centrality determination of p+Au collisions at 200 GeV. First: NGPT comparison between data and simulation; Second: Correlation between NGPT and $N_{\rm coll}$; Third: Centrality classes.

In p+Au collisions, R_{pAu} is the key quantity that is defined in a similar way as R_{AA} in section 3.1, with p+Au collisions replacing Au+Au in the numerator. Studying the R_{pAu} in different centrality classes can provide more differential information to distinguish between models. In order to obtain the R_{pAu} dependence on $N_{\rm part}$, we need to determine the centrality classes for p+Au collisions. We use track multiplicity in minimum-bias data at mid-rapidity (number of good primary tracks, NGPT) to classify p+Au collisions in centrality. The selection criteria for these tracks are the distance of closest approach to the primary vertex less than 1 cm, $|\eta| < 1$, and the number of TPC clusters used in track reconstruction being more than 10. The first panel of Fig. 2 shows the NGPT distribution from data and that from HIJING+GEANT simulation[10]. The NGPT distribution in data is well reproduced by the simulation. The second panel of Fig. 2 shows the correlation between the centrality determination variable (NGPT) and the number of binary nucleon-nucleon collisions. The last panel shows the three centrality classes used in this analysis along with the $\langle N_{\rm coll}\rangle$ values in these classes.

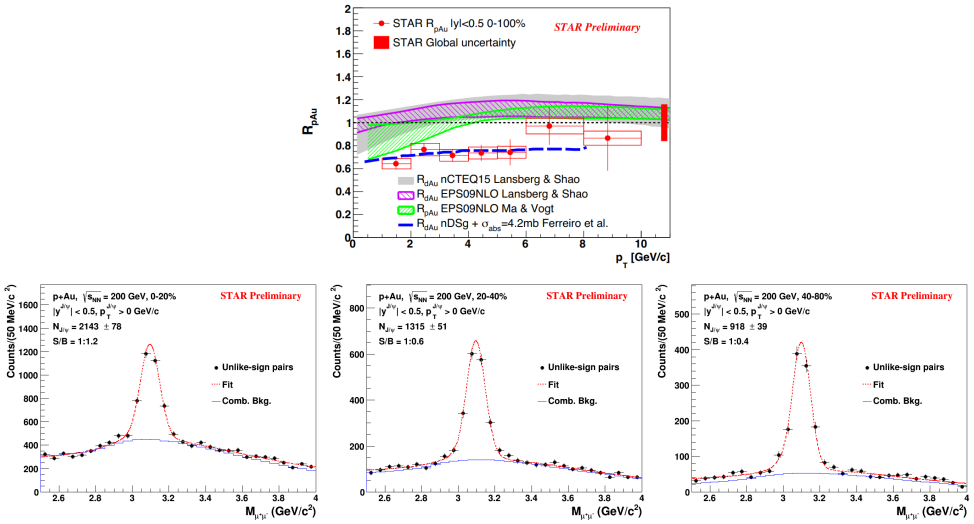

Fig. 3. Top: J/ψ R_{pA} as a function of p_T in p+Au collisions at 200 GeV in MB events. Bottom: the J/ψ signals in different centrality intervals.

The preliminary results for the J/ψ production in p+Au collisions are shown in Fig. 3. The top panel shows the minimum-bias (MB) results of R_{pAu} as a function of p_T. At high p_T ($p_T > 6$ GeV/c), the R_{pAu} is consistent with unity, while at low p_T, it is less than unity. Model calculations with the nPDFs effects [11] can touch data within uncertainties. Additional nuclear absorption [12] is favored by the data, which could have centrality dependence. Except for the statistical model (SHM), the models shown in Fig. 1 all include such additional nuclear absorption. The bottom three panels show the J/ψ signals in three centrality bins (0-20%, 20-40%, 40-80%) for p+Au collisions. In the future, we will use these data to obtain the R_{pA} as

a function of $N_{\rm part}$ and R_{pA} as a function of p_T in different centrality classes. Also, a measurement of the correlation between self-normalized yields and the event activity is underway.

3.3. J/ψ and Υ production in p+p collisions

In order to have a full picture of the J/ψ production in Au+Au and p+Au collisions, we also need to understand it in p+p collisions. In the first panel of Fig. 4, the self-normalized J/ψ yields versus the event activity (defined using charged-particle multiplicity) at mid-rapidity is shown for p+p collisions at $\sqrt{s}$ = 200 GeV. A stronger-than-linear rise is observed [13], in agreement with the ALICE measurement in p+p collisions at $\sqrt{s} = 7$ TeV. The second panel is again for the J/ψ, with comparisons to models. The percolation model and CGC/Saturation calculations are consistent with data [14, 15]. The model calculations have large discrepancy in the high-multiplicity range, therefore, more precise measurements at that region are needed to distinguish different models.

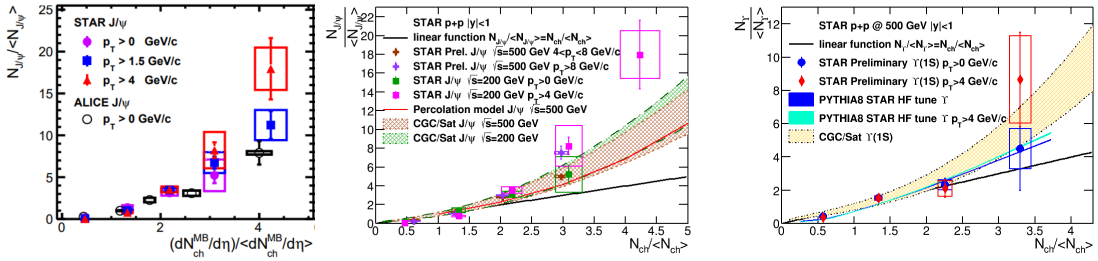

Fig. 4. First: the event activity for J/ψ with different p_T cuts compared to the ALICE result [13]. Second-Third: the event activity for J/ψ and $\Upsilon(1S)$ compared to the theoretical predictions.

We also looked at the $\Upsilon(1S)$ yields versus event activity in p+p collisions at $\sqrt{s}$ = 500 GeV and compared to the models as shown in the third panel in Fig. 4. The data trend can be described by the PYTHIA8 and CGC/Saturation models [14].

4. Conclusion

In Au+Au collisions, a strong suppression of J/ψ at high p_T is seen and the p_T dependence of the J/ψ R_{AA} are weak in all centrality classes. In p+Au collisions, there is a suppression at low p_T in the minimum-bias events, but the R_{pAu} is consistent with unity at high p_T. This indicates that in Au+Au collisions the suppression in the high p_T range is mainly from hot-medium effects. In p+p collisions, the dependences of both the J/ψ and Υ production on the charged-particle multiplicity at mid-rapidity at RHIC follow a faster-than-linear rise with multiplicity, similar to that seen at the LHC and they can be described by model predictions.

References

[1] T. Matsui and H. Satz, Phys. Lett. **B178**, 416 (1986).
[2] L. Grandchamp and R. Rapp, Phys. Lett. **B523**, 60 (2001).
[3] G. Bhanot and M. E. Peskin, Nucl. Phys. **B156**, 391 (1979).
[4] H. Paukkunen, Nucl. Phys. **A926**, 24 (2014).
[5] S. Gavin and R. Vogt, Phys. Rev. Lett. **78**, 1006 (1997).
[6] A. Capella, A. Kaidalov, A. Kouider Akil, and C. Gerschel, Phys. Lett. **B393**, 431 (1997).
[7] E. Ferreiro, Phys. Lett. B **749**, 98 (2015).
[8] STAR, J. Adam *et al.*, Phys. Lett. **B797**, 134917 (2019).
[9] X. Zhao and R. Rapp, Nucl. Phys. **A859**, 114 (2011).
[10] M. L. Miller, K. Reygers, S. J. Sanders, and P. Steinberg, Ann. Rev. Nucl. Part. Sci. **57**, 205 (2007).
[11] H.-S. Shao, Comput. Phys. Commun. **198**, 238 (2016).
[12] E. G. Ferreiro, F. Fleuret, J. P. Lansberg, N. Matagne, and A. Rakotozafindrabe, Few Body Syst. **53**, 27 (2012).
[13] STAR, J. Adam *et al.*, Phys. Lett. **B786**, 87 (2018).
[14] E. Levin and M. Siddikov, Eur. Phys. J. **C79**, 376 (2019).
[15] E. G. Ferreiro and C. Pajares, Phys. Rev. **C86**, 034903 (2012).